Published in final edited form as:
New Phytol. 2006 ; 171(1): 105–116. doi:10.1111/j.1469-8137.2006.01736.x.

Extraction of features from ultrasound acoustic emissions: a tool to assess the hydraulic vulnerability of Norway spruce trunkwood?

Sabine Rosner[1], **Andrea Klein**[2], **Rupert Wimmer**[2], and **Bo Karlsson**[3]

[1]Institute of Botany, Department of Integrative Biology, BOKU Vienna, Gregor Mendel Str. 33, A-1180 Vienna, Austria

[2]Institute of Wood Science and Technology, Department of Material Sciences and Process Engineering, BOKU Vienna, Peter Jordan Str. 62, A-1180 Vienna, Austria

[3]The Forestry Research Institute of Sweden (Skogforsk), Ekebo, S-26890 Svalöv, Sweden

Summary

• The aim of this study was to assess the hydraulic vulnerability of Norway spruce (*Picea abies*) trunkwood by extraction of selected features of acoustic emissions (AEs) detected during dehydration of standard size samples.

• The hydraulic method was used as the reference method to assess the hydraulic vulnerability of trunkwood of different cambial ages. Vulnerability curves were constructed by plotting the percentage loss of conductivity vs an overpressure of compressed air.

• Differences in hydraulic vulnerability were very pronounced between juvenile and mature wood samples; therefore, useful AE features, such as peak amplitude, duration and relative energy, could be filtered out. The AE rates of signals clustered by amplitude and duration ranges and the AE energies differed greatly between juvenile and mature wood at identical relative water losses.

• Vulnerability curves could be constructed by relating the cumulated amount of relative AE energy to the relative loss of water and to xylem tension. AE testing in combination with feature extraction offers a readily automated and easy to use alternative to the hydraulic method.

Keywords

acoustic emissions (AEs); cavitation; hydraulic vulnerability; peak amplitude; *Picea abies* (Norway spruce); signal energy; specific hydraulic conductance; trunkwood

Introduction

Milburn & Johnson (1966) were the first to detect cavitation events in plants by acoustic means using audio sound transducers and amplifiers in the low-frequency range (< 15 kHz). Tyree & Dixon (1983) adapted from engineering a more powerful tool for the acoustic detection of cavitations at frequencies between 100 and 2000 kHz, from which the Physical Acoustics Drought Stress Monitor (DMS) (Physical Acoustics Corporation, Princeton, NJ, USA) was later developed (Tyree & Sperry, 1989b). Because cavitations were detected over a very broad frequency range, the question soon arose whether the waveform characteristics

Author for correspondence: *Sabine Rosner Tel: +043 147654 3168 Fax: +043 147654 3180*rosner@edv1.boku.ac.at.

Europe PMC Funders Author Manuscripts

of acoustic emissions (AEs) carry any information about the hydraulic vulnerability of the conduits cavitated (Sandford & Grace, 1985; Ritman & Milburn, 1988, 1991; Tyree & Sperry, 1989a). In the present study, we attempted to filter out waveform characteristics from ultrasound AEs obtained during dehydration, such as peak amplitude, duration and relative energy, which can reliably describe the hydraulic vulnerability of Norway spruce (*Picea abies*) trunkwood.

Acoustic emissions with the highest amplitudes in the range of 100–300 kHz (Tyree & Sperry, 1989b) are probably induced by shock waves resulting from the sudden tension release in the conduit lumen as liquid water at negative pressure is replaced by water vapor very near vacuum pressure (Sandford & Grace, 1985; Tyree & Sperry, 1989a). The plant physiological application of AE testing is focused mainly on counting all AEs exceeding a defined detection threshold, on the assumption that the cumulated number of AEs corresponds to a loss of hydraulic conductivity (Tyree & Dixon, 1983; Tyree *et al.*, 1984a; Lo Gullo & Salleo, 1991; Cochard, 1992). AE counting is a reliable method of detecting periods of drought stress nondestructively, either in potted plants under controlled or open-air conditions (Peña & Grace, 1986; Salleo & Lo Gullo, 1986; Borghetti *et al.*, 1989; Tognetti & Borghetti, 1994; Jackson & Grace, 1996; Salleo *et al.*, 2000; Qiu *et al.*, 2002) or in mature trees directly in the field (Ikeda & Ohtsu, 1992; Jackson *et al.*, 1995; Jackson & Grace, 1996; Jackson *et al.*, 1999; Perks *et al.*, 2004; Hölttä *et al.*, 2005).

The construction of vulnerability curves (VCs) based on AE counting and the corresponding water potential or relative water content is complicated by the fact that any (dead) water-filled cell with walls rigid enough to resist collapse under negative pressure ought to be capable of cavitation (Tyree & Sperry, 1989a; Kikuta. 2003). AEs in conifer wood can thus originate from cavitating tracheids and ray tracheids, whereas in angiosperm wood they can originate from vessels, tracheids and fibers (Sandford & Grace, 1985; Tyree & Dixon, 1986). The cumulated rate of AEs is therefore not always proportional to the loss of hydraulic conductivity because cavitations of nonconductive cells are also counted. Even if each AE represents exactly one cavitation of a conduit (Tyree & Dixon, 1983; Tyree *et al.*, 1984a), the relation between cumulated AEs and conductivity loss will be nonlinear if not all the cells individually contribute the same amount to total hydraulic conductivity (Cochard, 1992). There is also no clear consensus regarding interpretation of the VCs. Whereas in some publications steeper slopes of VCs were interpreted as higher hydraulic vulnerability (Cochard, 1992; Hacke & Sauter, 1995; Hacke & Sauter, 1996), precisely the opposite relationship has been assumed by others (Tyree *et al.*, 1984a; Tyree & Dixon, 1986; Rosner, 2004; Rosner & Wimmer, 2005).

Interpretation of the VCs obtained by AE counting remains difficult, and more sophisticated analysis is needed to assess hydraulic vulnerability. One possible strategy is the extraction of the AE waveform information that is most closely related to the loss of hydraulic conductivity. It has been proposed by some authors that the energy or frequency composition of acoustic signals emitted by a cavitation event depends on the conduit dimensions (Milburn, 1973; Sandford & Grace, 1985; Ritman & Milburn, 1988, 1991). AE feature extraction is a well-established method in industrial lumber drying, where the analysis of the amplitude or energy distribution of AE signals has been successfully used to pinpoint wood checking (Niemz *et al.*, 1994; Lee *et al.*, 1996; Beall, 2002a; Kawamoto & Williams, 2002; Beall *et al.*, 2005). This methodological approach could be applied to physiological problems, because it is well known that the bulk of signals emitted during wood dehydration represent cavitations (Tyree *et al.*, 1984b; Quarles, 1992; Kawamoto & Williams, 2002). The filtering and analysis of the waveform features from the enormous number of ultrasound signals emitted during wood dehydration have become easier with the

development of appropriate software tools over the past decade (Beall, 2002a; Vallen, 2002).

The objective of this study was to test the reliability of AE waveform features, such as peak amplitude, AE duration and AE energy, for assessing the hydraulic vulnerability of Norway spruce trunkwood. Waveform features of the AEs emitted during dehydration of standard-size wood samples differing in anatomy and hydraulic vulnerability, namely juvenile and mature trunkwood (Brändström, 2001; Rosner, 2004; Rosner & Wimmer, 2005), were analyzed in detail. Additional anatomical investigations and VCs obtained using a hydraulic reference method, where hydraulic vulnerability was assessed by repeated flow measurements after application of air pressure on a similar sample set, were used to select AE features appropriate for the construction of VCs.

Materials and Methods

Plant material

Wood samples were taken from 25-year-old Norway spruce [*Picea abies* (L.) Karst.] trees that were part of a clonal trial in southern Sweden (Tönnersjöheden; latitude 56°67′, longitude 13°07′, 60 m above sea level). For the present study, four ramets of, in each case, three different clones were selected. They showed no significant differences in tree height (11.1 ± 0.4 m, $n = 12$) and diameter at breast height (13.3 ± 0.6 cm (mean ± SD), $n = 12$).

Sample harvesting and storage

All trees were harvested during a wet period in the middle of June 2004, when trees did not suffer from drought stress (14 June 2004). Trunkwood samples, 20–30 cm in length, were taken immediately after felling from the tree top (second internode), from the beginning of the crown, and at a height of 1 m above the ground. During transport, samples were kept wet in plastic bags containing some fresh water. In the laboratory the wood boles were debarked and split along the grain. An outer sapwood zone of 2 cm was separated from the split samples and placed in plastic zip bags together with fresh water containing 0.01% (by volume) Micropur (Katadyn Producte AG, Wallisellen, Switzerland). Whole internodes and beams were sent within 24 h to BOKU Vienna (Austria). Samples were stored frozen at −18°C until further preparation steps were carried out. Preliminary experiments on Norway spruce sapwood samples showed that freeze-storage of saturated samples for several weeks had no significant impact on specific hydraulic conductivity and vulnerability after thawing. Similar results were obtained by Mayr *et al.* (2003).

Preparation of standard beams for flow experiments and AE testing

Wood samples were thawed in fresh water for at least 3 h. Outer sapwood samples with a transverse surface of *c.* 0.9 × 0.9 cm were isolated by splitting the wood along the grain with a chisel. The tangential and radial faces of the beams were planed on a sliding microtome. Samples were shortened on a band saw, and sample ends were re-cut using a razor blade. During all these steps the wood samples were kept wet. They were then soaked in distilled water under vacuum for at least 48 h to refill embolized tracheids and afterwards stored in degassed water containing 0.01% (by volume) Micropur to prevent microbial growth. The final standard dimensions of the samples were 0.6 cm tangential, 0.6 cm radial, and 11.0 cm longitudinal. Standard beams were produced from samples taken at 1 m above the ground, comprising annual rings 17–19 (mature wood), and at the tree top, comprising annual rings 1–2 (juvenile wood).

Preparation of standard sections for AE testing

The method for testing wood sections for AEs was introduced by Kikuta *et al.* (2003). After thawing in fresh water for at least 3 h, small wood cubes (2 × 2 × 2 cm) were sawn from the samples. Radial sections 200 μm thick were cut on a sliding microtome. The area of the sections was reduced to a standard size of 13.3 mm (longitudinal) and 0.9 mm (radial) using a custom-made razor blade tool. Sections were only made from the earlywood of the outermost, completely developed annual rings of samples from the tree top (juvenile wood aged 1–2 years; $n = 16$), the beginning of the crown (young mature wood aged 13–14 years; $n = 15$) and 1 m above the ground (mature wood aged 17–19 years; $n = 15$) of one tree (diameter at breast height 12 cm; height 11 m). They were soaked in distilled water under vacuum for a few hours to remove all gas bubbles from the tracheids before AE testing. We chose earlywood for these experiments because similar tracheid lengths and lumen diameters were expected, permitting easier and more representative anatomical investigations.

Hydraulic method to assess hydraulic vulnerability

Specific hydraulic conductivity (k_s) describes the permeability of a wood segment following Darcy's law and is defined as:

$$k_s\left(\mathrm{m^2 s^{-1} MPa^{-1}}\right) = Q l A_s^{-1} \Delta P^{-1} \quad \text{Eqn 1}$$

[Q, the volume flow rate ($m^3\ s^{-1}$); l, the length of the segment (m); A_s, the sapwood cross-sectional area (m^2); ΔP, the pressure difference between the two ends of the segment (MPa).]

Conductivity data were corrected to 20°C to account for changes in fluid viscosity. Conductivity measurements were carried out under a hydraulic pressure head of 0.0054 MPa with distilled, filtered (0.22 μm), degassed water containing 0.005% (by volume) Micropur (Sperry *et al.*, 1988; Mayr, 2002). Vulnerability curves were obtained using methods described in Spicer & Gartner (1998) and Domec & Gartner (2001). After determination of the conductivity at full saturation ($k_{s(i)}$), air pressure (P) was applied to the lateral sides of the samples, while the transverse ends protruded from a double-ended pressure chamber (PMS Instruments Co., Corvallis, OR, USA), to induce cavitation. Following pressure treatment the samples were weighed and placed in distilled water for *c.* 30 min. Hydraulic conductivity ($k_{s(P)}$) was measured again after re-cutting the samples. Initially, the pressure chamber was pressurized to 0.5 MPa, and the pressure was subsequently increased after each conductivity measurement in steps of 0.5–1.0 MPa until more than 95% loss of conductivity (PLC) was reached. In some samples, the specific conductivity was up to 10% higher after exposure to low pressures between 0.5 and 1 MPa than the initial conductivity at full saturation. As a reference value for constructing vulnerability curves, the initial conductivity at full saturation was chosen, and flow rates measured after pressure application higher than the initial conductivity were excluded from the analysis. PLC at a given pressure (P) was calculated using the following equation:

$$\mathrm{PLC}\,(\%) = \left[\left(k_{s(i)} - l_{s(P)}\right)/k_{s(i)}\right] \times 100 \quad \text{Eqn 2}$$

Hydraulic vulnerability curves were fitted by the least squares method based on a sigmoidal function (Pammenter & Vander Willigen, 1998):

$$\mathrm{PLC}\,(\%) = 100/\{1+\exp[a(P-b)]\}, \quad \text{Eqn 3}$$

[a, the slope of the linear part of the curve; b, the potential at which 50 PLC occurred.]

The relative water loss (RWL) caused by the air overpressure was calculated as:

$$\mathrm{RWL}\,(\%) = [\,1 - (\text{actual fresh weight} - \text{dry weight}) / (\text{saturated weight} - \text{dry weight})\,] \times 100 \quad \text{Eqn 4}$$

Dry weight was obtained by drying wood samples at 103°C to constant weight.

RWL was related to the pressure applied (P) with the cubic function:

$$\mathrm{RWL}\,(\%) = b + b_1 P + b_2 P^2 + b_3 P^3 \quad \text{Eqn 5}$$

The dimensions of the standard beams were measured in the oven-dry state, and wood density was calculated as the dry weight divided by the volume in the oven-dry state. Hydraulic tests were performed on the samples taken at 1 m above the ground from the 12 trees harvested (mature wood samples) as well as on six samples prepared from the tree tops of two ramets per clone (juvenile wood samples), because material from the tree top was limited.

The acoustic method for the determination of hydraulic vulnerability

Acoustic emissions were monitored with the μDiSP™ Digital AE system from the Physical Acoustics Corporation (Princeton Jct, NJ, USA) (Sell, 2004). Preamplifiers (40 dB) were used in connection with resonant 150-kHz R15C transducers over a standard frequency range of 50–200 kHz. Data in the frequency range between 100 kHz and 1 MHz were recorded with a detection threshold of 30 dB (0 dB = 1 μV input), and with a sampling rate of 5 Msamples s^{-1} for the waveforms. The detection threshold was chosen as the peak amplitude of signals produced by waving the AE transducer in the air, plus 8–9 dB. Extraction of features such as the peak amplitude (dB), the AE duration (μs) and the relative AE energy (pVs) of each AE signal was carried out with AE Win® software (Physical Acoustics Corporation). Relative AE energy (also referred to as ‘PAC energy’) is defined as the area of the rectified voltage signal over the duration of the AE signal.

AE transducers were positioned on the tangential face of fully saturated standard beams or on standard-size sections using an acrylic resin clamp (Rosner & Wimmer, 2005). Silicone paste (Wacker, Burghausen, Germany) served as a coupling agent. A compression spring below the sample guaranteed a constant pressure of 30 ± 1 N (Jackson & Grace, 1996; Beall, 2002a) between transducer and wood. The samples were positioned on a metal disk fixed onto the compression spring. Pressure during the dehydration process was recorded with a DMS load cell (Type 8416-5500, range 0–500 N; amplification with an inline amplifier for DMS, Type 9235; Burster, Gernsbach, Germany) between the AE transducer and the screw of the acrylic resin clamp. The acrylic resin clamp was kept deep enough in the water that the wood sample was totally covered until the applied pressure reached a constant value. After quickly removing superficial water from the clamp and the wood, recording of AEs and coupling pressure was started. Water loss of the standard beams at ambient temperature (22°C at 40% relative humidity) was quantified by placing the whole clamp assemblage on a balance (resolution 10^{-3} g; Sartorius, Göttingen, Germany) and reading the weight every 10 min. AE testing was continued until no more signals were emitted, which was the case after *c.* 10–12 h for the standard beams, and after 2 h for the standard sections.

AE data filtering was achieved with Vallen VisualAE™ software (Vallen Systeme GMbH, Munich, Germany). AE signals with lower peak amplitudes than 30.5 dB were filtered out from the data set. Signals with peak amplitudes lower than 30.5 dB corresponded to signals that passed the detection threshold of 30 dB only once and were interpreted using their waveform as signals which originated from the system itself or from background noise. AE

data were then clustered into amplitude (PA_{AE}) ranges: 30.5 dB ≤ PA_{AE} < 40 dB, 40 dB ≤ PA_{AE} < 50 dB, 50 dB ≤ PA_{AE} < 60 dB, and PA_{AE} ≥ 60 dB. AE data were also clustered by AE duration (D_{AE}): D_{AE} < 100 μs, 100 μs ≤ D_{AE} < 500 μs, and D_{AE} ≥ 500 μs. A mean AE energy value was calculated for 10-min time-steps (AE energy/10 min). Relative cumulated AE energy data were obtained by relating the stepwise cumulated AE energy/10 min to the sum of AE energy/10 min. Relative water loss during dehydration of the standard beams and AE signals were related to each other in 10-min time-steps (AEs/10 min). Clustered AEs/10 min and AE energy/10 min were then referred to the nearest 5% RWL step to allow statistical analysis. 'AE rates' are the clustered AEs/10 min related to maximum clustered AEs/10 min, and 'relative AE rates' are the clustered AEs/10 min related to all AE signals detected during the same time interval.

Vulnerability curves based on the cumulated AEs or AE energies during water loss were fitted by a cubic function:

$$\text{Cumulative AEs}\,(\%) = b + b_1\text{RWL} + b_2\text{PWL}^2 + b_3\text{RWL}^3 \quad \text{Eqn 6}$$

AE feature extraction and data clustering were carried out for 12 juvenile and mature standard beams, respectively, originating from four ramets of three different clones.

Anatomical investigations after AE testing

After AE testing, all standard sections were placed in a mixture of alcohol, water and glycerol (1 : 1 : 1) for 1 d. On a sliding microtome, 20-μm transverse sections were cut at each end of the standard sections, stained with methylene blue, dehydrated, and mounted in Entellan (Merck, Darmstadt, Germany). The number of nonsevered tracheids (whole radial and tangential cell wall intact) was recorded by counting under a microscope. The remaining tissue was macerated in Jeffrey's solution (Jeffrey, 1917). Tracheid length was measured using National Institutes of Health (NIH) image software (freely available from http://rsb.info.nih.gov). Mean tracheid length was calculated from 40 measurements on every 200-μm standard section. The number of nonsevered tracheids per standard section (N_T) was calculated as:

$$N_T = (L - l)\, l^{-1} n_T \quad \text{Eqn 7}$$

[L, the longitudinal dimension of the standard section (13.3 mm); l, the mean tracheid length; n_T, the number of nonsevered tracheids on the transverse face of the standard section.]

Transverse sectioning of the 200-μm standard sections was also used to identify and exclude samples that were not cut exactly radially, contained some latewood or deviated strongly from 200 μm in the tangential direction.

Transversally cut faces of the sites where the AE transducer was clamped onto the standard beams were sanded and the number of tracheids within a window of 0.33 mm (radial) and 0.48 mm (tangential) was recorded by counting under a microscope. Tracheid counts were performed in the earlywood regions only.

Statistics

Statistical analysis was carried out with SPSS® 11.0 (SPSS Inc., Chicago, IL, USA). Values are given as mean ± standard error (SE). Mean values were tested for significance with the t-test for independent samples, after analysis of variance and checking for normal distribution. Associations between two variables were examined using linear or nonlinear regression

analysis. In the tables, significant differences between variables are indicated by different letters. Differences between mean values and relationships were accepted as significant if P was < 0.05 (*, $P < 0.05$; **, $P < 0.01$; ***, $P < 0.001$).

Results

Flow experiments

Juvenile wood was more resistant to cavitation than mature wood (Fig. 1a); a 50% loss of conductivity (PLC) required 3.20 ± 0.16 MPa air pressure, whereas a pressure of only 2.26 ± 0.04 MPa produced the same effect in mature wood ($P < 0.001$). Comparison of the overpressures resulting in 50% RWL revealed similar differences (juvenile, 3.67 ± 0.17 MPa; mature, 2.58 ± 0.06 MPa; $P < 0.001$; Fig. 1b). The slopes of PLC vs RWL were quite similar in juvenile and mature samples (data not shown); 50 PLC was reached in juvenile wood at 39.88 ± 1.48% RWL, and in mature wood at 35.97 ± 0.85% RWL ($P < 0.05$). Juvenile samples had significantly lower maximum specific conductivities than mature samples (4.99 ± 0.90 and 37.21 ± 1.55 $cm^2\ s^{-1}\ MPa^{-1}$, respectively; $P < 0.001$). The water content at full saturation as a percentage of dry weight was slightly higher in mature than in juvenile wood (225.4 ± 7.4% and 193.5 ± 17.4%, respectively; $P < 0.05$), but wood density showed no differences between juvenile and mature wood (0.41 ± 0.01 and 0.38 ± 0.01 g cm^{-3}, respectively).

Number of cumulated AEs and tracheid number

The number of tracheids was strongly correlated with the number of AEs from defined earlywood regions (standard sections; Fig. 2). Juvenile wood sections had much higher tracheid numbers mm^{-3} (568.0 ± 38.5 and 201.4 ± 13.62, respectively; $P < 0.001$) and total AEs (2309.6 ± 125.2 and 608.6 ± 33.3, respectively; $P < 0.001$) than mature sections. Beams of juvenile wood also produced more AEs and had higher numbers of earlywood tracheids mm^{-2} than those of mature wood (Table 1). Total AEs were therefore positively correlated to the number of earlywood tracheids mm^{-2} ($r = 0.91$, $P < 0.001$).

Rate of total acoustic emissions

Acoustic emissions started in juvenile wood beams at slightly smaller RWLs than in mature beams (6.60 ± 0.89% and 8.72 ± 0.56%, respectively; $P < 0.01$). Juvenile wood also showed a higher rate of cumulated AEs per unit water loss. In juvenile wood beams, 50% cumulative AEs corresponded to 64.60 ± 1.73% RWL, whereas in mature wood this corresponded to as much as 72.84 ± 2.31% RWL ($P < 0.01$; Fig. 3b). The AE rate/10 min in juvenile wood showed a continuous rise, whereas in mature wood two peaks were observed at the beginning and towards the end of dehydration (Fig. 3a).

AE features

Peak amplitude—Signals with AE peak amplitudes (PA_{AE}) between 30 and 50 dB made up more than 85% of all signals detected on wood beams (Table 1). Therefore, their rates corresponded more or less to the general slope of the AE rate during dehydration (Figs 3a, 4a,b). Signals between 50 and 60 dB showed their highest rates at the beginning and towards the end of dehydration in mature wood, whereas in juvenile wood their rate did not decrease after the first peak (Fig. 4c). AEs with peak amplitudes > 60 dB were very rare (Fig. 4h), but their percentage was significantly higher in mature wood (Table 1) and negatively correlated to the total number of AEs ($r = -0.66$, $P < 0.001$). Maximum rates of AEs with peak amplitudes over 60 dB were found later in juvenile than in mature wood (30.24 ± 3.06% and 22.75 ± 1.96%, respectively; $P < 0.05$; Fig. 4d). Their number related to the total number of AEs between 20 and 30% of RWL was also much higher in mature wood than in juvenile

wood, as was the case for signals between 50 and 60 dB (Fig. 4g–h). Maximum relative rates of signals > 60 dB occurred at higher relative water losses in juvenile than in mature wood (30.29 ± 3.07% and 22.34 ± 1.52%, respectively; $P < 0.05$). The cumulated AE rate of signals > 60 dB was therefore significantly higher in mature than in juvenile wood at RWL between 25 and 35% (Fig. 3c).

Duration—Whereas juvenile beams produced more signals < 100 μs and > 500 μs, mature beams emitted a significantly higher percentage of signals between 100 and 500 μs throughout the whole dehydration period (Table 1, Fig. 5d–f). The total number of AEs was correlated negatively with the percentage of AEs between 100 and 500 μs ($r = -0.89$, $P < 0.001$), but positively with the percentage of AEs < 100 μs ($r = 0.74$, $P < 0.001$) and > 500 μs ($r = 0.97$, $P < 0.001$). Mature wood had significantly lower rates of AEs < 500 μs between 30 and 70% RWL (Fig. 5a–b) and higher rates of AEs > 500 μs between 25 and 30% RWL than juvenile wood (Fig. 5c).

Energy—The mean relative AE energy/10 min was significantly higher in mature than in juvenile beams (0.50 ± 0.03 and 0.29 ± 0.03 pV, respectively; $P < 0.001$). Mean AE energy/10 min corresponded negatively to the number of earlywood tracheids mm^{-2} ($r = -0.77$, $P < 0.001$) and to the total number of AEs ($r = -0.79$, $P < 0.001$). Maximum AE energy/10 min was negatively correlated to the number of earlywood tracheids mm^{-2} ($r = -0.60$, $P < 0.01$) and to the total number of AEs ($r = -0.87$, $P < 0.001$), because juvenile wood showed much lower maximum AE energy values ($P < 0.001$; Fig. 6a). Signals with maximum energies were emitted after significantly higher RWL in juvenile than in mature wood (30.61 ± 3.24% and 22.86 ± 1.59%, respectively; $P < 0.05$). The relative rates of the cumulated energy had significantly steeper slopes in mature than in juvenile wood (Fig. 6b) and 50% of the total amount of energy emitted was reached at lower RWL in mature than in juvenile wood (39.37 ± 2.15% and 50.99 ± 2.53%, respectively; $P < 0.001$). The pressure application necessary to produce 50% of the cumulated AE energy, as derived from RWL by Eqn 5, was much lower in mature than in juvenile wood (2.31 ± 0.05 and 3.73 ± 0.11 MPa, respectively; $P < 0.001$). Presentation of the model VCs based on cumulated energy vs pressure application in Fig. 1c allows comparison with the VCs obtained by the hydraulic method (Fig. 1a).

Discussion

Hydraulic vulnerability assessed by flow experiments

Juvenile wood of Norway spruce was less sensitive to cavitation, released less water at identical pressures and showed a lower specific hydraulic conductivity than mature wood (Fig. 1). Similar results obtained with the hydraulic method have also been reported for other conifer species (Domec & Gartner, 2001, 2003). The low values of b (pressure to achieve 50% loss of conductivity; Eqn 3) for mature wood indicate wide pit membrane pores in the tracheids. High values of a (an indicator of the slope of the linear part of the vulnerability curve; Eqn 3) in mature wood suggest a narrow range in maximum pore sizes across tracheids (Pammenter & Vander Willigen, 1998). On the basis of these results, we could attempt to filter out physiological information from acoustic emissions during wood dehydration.

Acoustic emissions and tracheid number

Acoustic emissions from earlywood sections were strongly correlated with the number of tracheids (Fig. 2). The number of AEs exceeded the number of tracheids by a factor of 1.7. In earlier studies, conduit numbers were found to be higher than the numbers of AEs (Sandford & Grace, 1985), or in a 1 : 1 relationship, so that each AE represented one

cavitation event (Tyree & Dixon, 1983; Tyree *et al.*, 1984a; Cochard, 1992). The higher number of AEs in relation to tracheid number could be a result of the sensitivity of the digital acoustic equipment which may detect cavitations of ray tracheids, as well as reflections of waves from internal surfaces, and small drying checks in the late dehydration period. The peak of the overall AE rate during the late drying period (Fig. 3a) corresponded to RWL around the 'fiber saturation point' (Rosner & Wimmer, 2005), where the cell lumina contain no water, but walls are fully saturated with liquid (Skaar, 1988; Berry & Roderick, 2005). At the fiber saturation point a shrinkage process starts, which can induce small drying checks (Kawamoto & Williams, 2002). The attenuation and thus the number of AEs detected also depend strongly on the contact pressure between the transducer and the wood sample (Beall, 2002b; Kikuta *et al.*, 2004), which makes it difficult to relate each AE to a single cavitation event. A 1 : 1 relationship might be calibrated for the coupling pressure used by varying the detection threshold, whereas we preferred to detect all signals before we filtered out reliable waveform information.

Hydraulic vulnerability assessed by AE feature extraction

Juvenile trunkwood showed a higher rate of cumulated AEs per unit of RWL than mature wood (Fig. 3b). Steeper slopes of VCs based on cumulated AEs were interpreted as lower hydraulic vulnerability in some species (Tyree *et al.*, 1984a; Tyree & Dixon, 1986; Rosner & Wimmer, 2005). The differences in the slopes were significant after 50% RWL, which is very late from a physiological point of view, because a RWL of only 35–40% leads to 50% loss of hydraulic conductivity. The bulk of AEs were produced after 50% RWL, as also observed in other conifer species (Tyree & Dixon, 1986). Signals at RWL > 70% may come from cavitation events in tracheids which contribute less to axial water transport than to other wood functions such as radial water transport, mechanical support (Gartner, 1995), and storage of water (Sandford & Grace, 1985; Holbrook, 1995), or from cavitations in ray tracheids and mechanical failure. However, almost linear relationships between loss of conductivity and cumulated AEs have been observed in Norway spruce branches (Cochard, 1992; Rosner, 2004). Plotting all cumulated AEs against relative water loss or xylem tension can be an appropriate method to assess the hydraulic vulnerability in branch samples, whereas for Norway spruce trunkwood a more reliable analysis method is needed to construct VCs.

We focused the search for parameters to assess hydraulic vulnerability on AE feature clusters which showed significantly different peak rates between juvenile and mature wood at moderate water losses. The rates of AEs clustered by the duration ranges showed differences between juvenile and mature wood throughout the dehydration period, but no differences in peak rates were found, except with signals > 500 μs at small water losses (Fig. 5a–c). These differences in the peak rates were too small to allow assessment of hydraulic vulnerability. Age-dependent differences in peak rates and relative peak rates of signals > 60 dB were very pronounced during the early stages of dehydration (Fig. 4d,h). Although there were significant differences in the steepness of the slopes of the cumulated AEs > 60 dB between juvenile and mature wood between 25 and 35% RWL (Fig. 3c), relating the RWL to the cumulated AEs by a cubic function resulted in no significant differences in RWL for any cumulated AE range. Raising the AE detection threshold does not seem appropriate to obtain reliable VCs, especially as signals > 60 dB comprise < 4% of all AEs (Table 1).

The relative AE energy contains information about both duration and peak amplitude, and therefore maximum energy values were reached later in juvenile than in mature wood (Fig. 6a). Plotting the cumulated AE energy/10 min related to the total energy emitted/10 min against the RWL gave the most promising results for assessing the hydraulic vulnerability of Norway spruce trunkwood. The relative rate of the cumulated energy had significantly steeper slopes in mature wood than in juvenile wood even at moderate water losses, and

therefore the RWL corresponding to 50% of the cumulated amount of energy was significantly smaller in mature than in juvenile wood samples (Fig. 6b). A model VC in which the cumulated energy was directly related to xylem tension (positive pressure application calculated from RWL in a parallel sample set) underlined the high information potential of this AE parameter for assessing hydraulic vulnerability (Fig. 1c). A much lower pressure application was necessary for 50% cumulated AE energy in mature than in juvenile wood. Differences in the steepness of the slopes between juvenile and mature wood became even more obvious, because in mature wood less pressure was necessary to remove the same relative amount of water compared with juvenile wood. In mature wood, the positive pressure to induce 50% cumulated energy corresponded exactly to 50 PLC (2.3 MPa), whereas in juvenile wood this stage was reached at xylem tensions corresponding to 50% RWL (3.7 MPa).

VCs based on cumulated AE energy are strong evidence that cavitations of more vulnerable, large-diameter tracheids emit stronger AEs than those of less vulnerable tracheids, and thus that larger conduits store more elastic energy when under tension (Milburn, 1973; Sandford & Grace, 1985; Ritman & Milburn, 1988, 1991). Within a species, the vulnerability of a tracheid to embolism is a direct function of its diameter and pit pore characteristics (Lo Gullo & Salleo, 1991; Cochard, 1992; Hacke & Sperry, 2001; Mayr *et al.*, 2002; Tyree & Zimmermann, 2002), and therefore earlywood tracheids are thought to be the first to cavitate (Tyree *et al.*, 1984a; Tyree & Sperry, 1989a). Lumen diameters of Norway spruce tracheids decrease within an annual ring from earlywood to latewood and increase with cambial age (Brändström, 2001). The density of bordered pits increases with tracheid lumen diameter (Sirviö & Kärenlampi, 1998). We found two to three times higher tracheid numbers in juvenile (1–2-year) than in mature (17–19-year) Norway spruce earlywood, implying smaller conduit dimensions in juvenile than in mature wood. The cavitation of a small number of very large (and thus very vulnerable) tracheids may have a dramatic effect on conductivity, as flow rate is proportional to the 4th power of the radius of a capillary (Hagen–Poiseuille equation). The distribution of maximum AE energies suggests that cavitation of the most vulnerable tracheids occurred at lower RWL or xylem tension in mature than in juvenile samples (Figs 1b,c, 6a). The highest energy values were not found right at the beginning of dehydration, a finding also obtained by Tyree *et al.* (1984a). AEs started after *c.* 5–10% RWL, because tensions sufficient to cause cavitations can only develop when all the water from severed tracheids at the cut faces of the sample has evaporated (Tyree *et al.*, 1984a; Sandford & Grace, 1985; Tyree & Dixon, 1986). This point was reached at slightly lower water losses in juvenile samples, because tracheid dimensions were smaller. Weak signals shorter than 100 μs (Fig. 5d) and with amplitudes < 40 dB (Fig. 4e) did not cause an immediate loss of conductivity, and are thought to arise from cavitation events of capillary water (Tyree & Dixon, 1986; Tyree & Zimmermann, 2002). Perks *et al.* (2004) recently calculated that even cavitation of 15% of tracheids does not affect hydraulic conductance in *Pinus sylvestris*.

Analysis of AE features can be a useful tool to separate harmful (impairing conductivity) from less harmful cavitations, but its application is restricted to laboratory conditions and standard-size samples have to be small enough to be within the listening distance of the transducer but big enough to enable recording of the water loss on a balance. We believe that our AE results give reliable information about the conduits cavitated over the entire transverse face, because the tangential and radial dimensions of the standard beams were small enough to be within the listening distance of the transducer (Tyree *et al.*, 1984a; Sandford & Grace, 1985; Ritman & Milburn, 1991; Jackson & Grace, 1996), which minimized errors associated with attenuation. Wood density is known to affect attenuation of AE signals negatively (Ritman & Milburn, 1988; Tyree & Sperry, 1989a,b; Jackson & Grace, 1996); however, in the samples investigated no relationships between density and AE

peak amplitude or energy were found. Water content at full saturation was lower in juvenile wood samples. High water content can influence sound propagation negatively (Ritman & Milburn, 1988; Tyree & Sperry, 1989a; Quarles, 1990; Jackson & Grace, 1996; Beall, 2002a), but the mean AE energy showed higher values in mature than in juvenile wood throughout the dehydration period.

Analysis of the spectrum features of AE signals during wood dehydration offered an interesting alternative to the hydraulic method for assessing the hydraulic vulnerability of Norway spruce trunkwood. VCs were constructed by relating the relative cumulated amount of AE energy during dehydration of standard beams under defined conditions to the RWL. The measurement of RWL and corresponding positive pressure application in a parallel sample set enables the construction of model VCs, where the cumulated AE energy can be related to xylem tension. The RWL or the xylem tension corresponding to 50% of the cumulated energy emitted can be a useful parameter to quantify hydraulic vulnerability. The major advantage of the AE method presented is that it is readily automated and easier to use than the hydraulic method.

Acknowledgments

This study was financed by the Austrian Science Fund FWF (Project P16275-B06). We thank Gudmund Ahlberg for technical assistance in the field and Joachim Sell for technical advice and helpful discussions. Hanno Richter is thanked for critical reading of the manuscript and for linguistic corrections. Suggestions by two anonymous referees helped us to improve an earlier version of this paper.

References

Beall FC. Overview of the use of ultrasonic technologies in research on wood properties. Wood Science and Technology. 2002a; 36:197–212.

Beall, FC. Acoustic emission and acousto-ultrasonics. Nondestructive testing of wood. Forest Products Society; Madison, WI, USA: 2002b. p. 37-48.

Beall FC, Breiner TA, Wang J. Closed-loop control of lumber drying based on acoustic emission peak amplitude. Forest Products Journal. 2005; 55:167–174.

Berry SL, Roderick ML. Plant-water relations and the fibre saturation point. New Phytologist. 2005; 168:25–38. [PubMed: 16159318]

Borghetti M, Raschi A, Grace J. Ultrasound emission after cycles of water stress in *Picea abies*. Tree Physiology. 1989; 5:229–237. [PubMed: 14972990]

Brändström J. Micro- and ultrastructural aspects of Norway spruce tracheids: a review. IAWA Journal. 2001; 22:333–353.

Cochard H. Vulnerability of several conifers to air embolism. Tree Physiology. 1992; 11:73–83. [PubMed: 14969968]

Domec J-C, Gartner BL. Cavitation and water storage in bole segments of mature and young Douglas-fir trees. Trees. 2001; 15:204–214.

Domec J-C, Gartner BL. Relationship between growth rates and xylem hydraulic characteristics in young, mature and old-growth ponderosa pine trees. Plant, Cell & Environment. 2003; 26:471–483.

Gartner, BL. Patterns of xylem variation within a tree and their hydraulic and mechanical consequences. In: Gartner, BL., editor. Plant stems: physiology and functional morphology. Academic Press; New York, NY, USA: 1995. p. 125-149.

Hacke U, Sauter JJ. Vulnerability of xylem to embolism in relation to leaf water potential and stomatal conductance in *Fagus sylvatica* f. *purpurea* and *Populus balsamifera*. Journal of Experimental Botany. 1995; 46:1177–1183.

Hacke U, Sauter JJ. Drought-induced xylem dysfunction in petioles, branches, and roots of *Populus balsamifera* L. and *Alnus glutinosa* (L.) Gaertn. Plant Physiology. 1996; 111:413–417. [PubMed: 12226296]

Hacke UG, Sperry JS. Functional and ecological xylem anatomy. Perspectives in Plant Ecology, Evolution and Systematics. 2001; 4:97–115.

Holbrook, NM. Stem water storage. In: Gartner, BL., editor. Plant stems: physiology and functional morphology. Academic Press; New York, NY, USA: 1995. p. 105-124.

Hölttä T, Vesala T, Nikinmaa E, Perämäki M, Siivola E, Mencuccini M. Field measurements of ultrasonic acoustic emissions and stem diameter variations. New insight into the relationship between xylem tensions and embolism. Tree Physiology. 2005; 25:237–243. [PubMed: 15574405]

Ikeda T, Ohtsu M. Detection of xylem cavitation in field-grown pine trees using the acoustic emission technique. Ecological Research. 1992; 7:391–395.

Jackson GE, Grace J. Field measurements of xylem cavitation: are acoustic emissions useful? Journal of Experimental Botany. 1996; 47:1643–1650.

Jackson GE, Irvine J, Grace J. Xylem cavitation in two mature Scots pine forests growing in a wet and a dry area of Britain. Plant, Cell & Environment. 1995; 18:1411–1418.

Jackson GE, Irvine J, Grace J. Xylem acoustic emissions and water relations of *Calluna vulgaris* L. at two climatological regions of Britain. Plant Ecology. 1999; 140:3–14.

Jeffrey, EC. The anatomy of woody plants. University of Chicago Press; Chicago, IL, USA: 1917.

Kawamoto, S.; Williams, RS. Acoustic emission and acousto-ultrasonic techniques for wood and wood-based composites: a review. U.S. Department of Agriculture, Forest Service, Forest Products Laboratory; Madison, WI, USA: 2002. General Technical Report FPL-GTR-134

Kikuta SB. Utrasound acoustic emissions from bark samples differing in anatomical characteristics. Phyton (Horn, Austria). 2003; 43:161–178.

Kikuta SB, Hietz P, Richter H. Vulnerability curves from conifer sapwood sections exposed over solutions with known water potentials. Journal of Experimental Botany. 2003; 54:2149–2155. [PubMed: 12867547]

Kikuta, SB.; Lo Gullo, MA.; Kartusch, B.; Rosner, S.; Richter, H. Ultrasound acoustic emissions from conifer sapwood sections: relationship between number of events detected and number of tracheids. In: Barnet, JR., editor. Proceedings of the IAWA International Symposium on Wood Sciences; Montpellier, France. 24–29 October, 2004; IAWA; 2004. p. 30-31.

Lee S-H, Quarles SL, Schniewind AP. Wood fracture, acoustic emission, and drying process. Part 2. Acoustic emission pattern recognition analysis. Wood Science and Technology. 1996; 30:283–292.

Lo Gullo MA, Salleo S. Three different methods for measuring xylem cavitation and embolism: a comparison. Annals of Botany. 1991; 67:417–424.

Mayr S. A modified Sperry-Apparatus for measuring embolism in the xylem of trees. Berichte des naturwissenschaftlichen medizinischen verein Innsbruck. Verein Innsbruck. 2002; 89:99–110.

Mayr S, Gruber A, Bauer H. Repeated freeze–thaw cycles induce embolism in drought stressed conifers (Norway spruce, stone pine). Planta. 2003; 217:436–441. [PubMed: 14520570]

Mayr S, Wolfschweger M, Bauer H. Winter-drought induced embolism in Norway spruce (*Picea abies*) at the Alpine timberline. Physiologia Plantarum. 2002; 115:74–80. [PubMed: 12010469]

Milburn JA. Cavitation in *Ricinus* by acoustic detection: Induction in excised leaves by various factors. Planta. 1973; 110:253–265.

Milburn JA, Johnson RPC. The conduction of sap. I. Detection of vibrations produced by sap cavitation in *Ricinus* xylem. Planta. 1966; 69:43–52.

Niemz P, Emmler R, Pridöhl E, Fröhlich J, Lühmann A. Vergleichende Untersuchungen zur Anwendung von piezoelektrischen und Schallemissionssignalen bei der Trocknung von Holz. Holz Als Roh- und Werkstoff. 1994; 52:162–168.

Pammenter NW, Vander Willigen C. A mathematical and statistical analysis of the curves illustrating vulnerability of xylem to cavitation. Tree Physiology. 1998; 18:589–593. [PubMed: 12651346]

Peña J, Grace J. Water relations and ultrasound emissions of *Pinus sylvestris* before, during and after periods of water stress. New Phytologist. 1986; 103:515–524.

Perks MP, Irvine J, Grace J. Xylem acoustic signals from mature *Pinus sylvestris* during an extended drought. Annals of Forest Science. 2004; 61:1–8.

Qiu GY, Okushima L, Sase S, Lee I-B. Acoustic emissions in tomato plants under water stress conditions. Japan Agricultural Research Quarterly. 2002; 36:103–109.

Quarles SL. The effect of moisture content and ring angle on the propagation of acoustic signals in wood. Journal of Acoustic Emission. 1990; 9:189–195.

Quarles SL. Acoustic emission associated with oak during drying. Wood and Fiber Science. 1992; 24:2–12.

Ritman KT, Milburn JA. Acoustic emissions from plants: ultrasonic and audible compared. Journal of Experimental Botany. 1988; 38:1237–1248.

Ritman KT, Milburn JA. Monitoring of ultrasonic and audible emissions from plants with or without vessels. Journal of Experimental Botany. 1991; 42:123–130.

Rosner S. Acoustic detection of cavitation events in water conducting elements of Norway spruce sapwood. Journal of Acoustic Emission. 2004; 22:110–118.

Rosner, S.; Wimmer, R. Acoustic detection of cavitation events in Norway spruce sapwood. In: Bröker, F-W., editor. 14th International Symposium on Nondestructive Testing of Wood. Shaker Verlag; Aachen, Germany: 2005. p. 123-134.

Salleo S, Lo Gullo MA. Xylem cavitation in nodes and internodes of whole *Chorisia insignis* H.B. et K. plants subjected to water stress: Relations between xylem conduit size and cavitation. Annals of Botany. 1986; 58:431–441.

Salleo S, Nardini A, Pitt F, Lo Gullo MA. Xylem cavitation and hydraulic control of stomatal conductance in Laurel (*Laurus nobilis* L.). Plant, Cell & Environment. 2000; 23:71–79.

Sandford AP, Grace J. The measurement and interpretation of ultrasound from woody stems. Journal of Experimental Botany. 1985; 36:298–311.

Sell J. Overview of new Acoustic Emission (AT) Systems, PAC Developments. Deutsche Gesellschaft für zerstörungsfreie Prüfung e.V. Berichtsband. 2004; 90(2):803–810.

Sirviö J, Kärenlampi P. Pits as natural irregularities in softwood fibers. Wood and Fiber Science. 1998; 30:27–39.

Skaar, C. Wood–water relations. Springer-Verlag; Berlin, Germany: 1988.

Sperry JS, Donnelly JR, Tyree MT. A method for measuring hydraulic conductivity and embolism in xylem. Plant, Cell & Environment. 1988; 11:35–40.

Spicer R, Gartner BL. Hydraulic properties of Douglas-fir (*Pseudotsuga menziesii*) branches and branch halves with references to compression wood. Tree Physiology. 1998; 18:777–784. [PubMed: 12651412]

Tognetti R, Borghetti M. Formation and seasonal occurrence of xylem embolism in *Alnus cordata*. Tree Physiology. 1994; 14:241–250. [PubMed: 14967699]

Tyree MT, Dixon MA. Cavitation events in *Thuja occidentalis* L.? Ultrasonic acoustic emissions from the sapwood can be measured. Plant Physiology. 1983; 72:1094–1099. [PubMed: 16663126]

Tyree MT, Dixon MA. Water stress induced cavitation and embolism in some woody plants. Physiologia Plantarum. 1986; 66:397–405.

Tyree MT, Dixon MA, Thompson RG. Ultrasonic acoustic emissions from the sapwood of *Thuja occidentalis* measured inside a pressure bomb. Plant Physiology. 1984b; 74:1046–1049. [PubMed: 16663501]

Tyree MT, Dixon AD, Tyree EL, Johnson R. Ultrasonic acoustic emissions from the sapwood of cedar and hemlock. An examination of three hypothesis regarding cavitations. Plant Physiology. 1984a; 75:988–992. [PubMed: 16663774]

Tyree MT, Sperry JS. Vulnerability of xylem to cavitation and embolism. Annual Review of Plant Physiology and Plant Molecular Biology. 1989a; 40:19–38.

Tyree MT, Sperry JS. Characterization and propagation of acoustic emission signals in woody plants: towards an improved acoustic emission counter. Plant, Cell & Environment. 1989b; 12:371–382.

Tyree, MT.; Zimmermann, MH. Xylem structure and the ascent of sap. 2nd edn. Springer; Berlin, Germany: 2002.

Vallen H. AE testing fundamentals, equipment, applications. NDT.Net. 2002; 7:1–29.

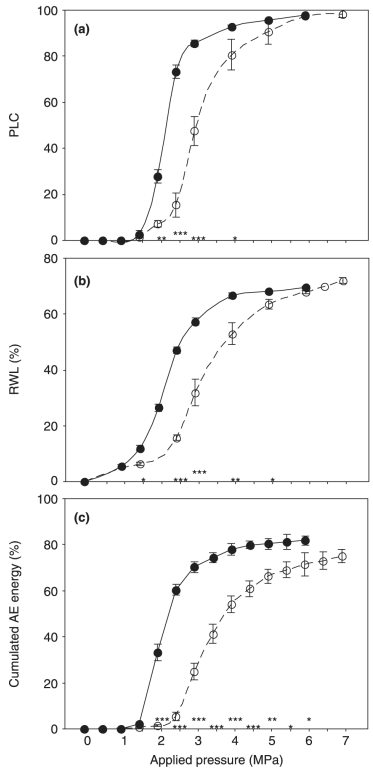

Fig. 1.

Per cent loss of conductivity (PLC) (a), relative water loss (RWL) (b), and relative cumulated acoustic emission (AE) energy (c) related to overpressures applied with a pressure collar. X-scale data for (c) were derived from cubic fit models (Eqn 5), where the RWL was related to the overpressure applied. Error bars represent 1 standard error (SE). Open symbols and dashed lines represent juvenile sapwood beams [(a, b) $n = 6$; (c) $n = 12$)]; closed symbols and solid lines represent mature sapwood beams ($n = 12$). Values of a (Fig. 1a, Eqn 3) were 1.82 ± 0.25 (mean ± SE) in juvenile wood and 3.44 ± 0.27 in mature wood ($P < 0.001$). Differences between juvenile and mature samples are marked with * at the corresponding pressure if significant at the 0.05 level, with ** if significant at the 0.01 level, and with *** if significant at the 0.001 level.

Europe PMC Funders Author Manuscripts

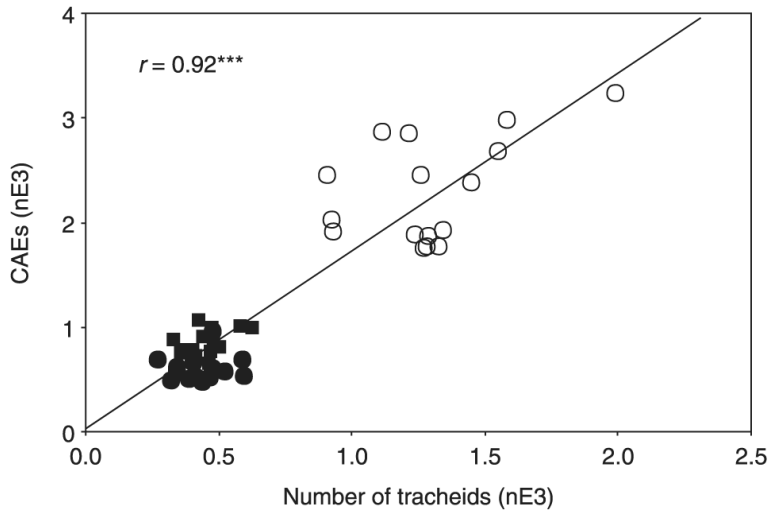

Fig. 2.

Cumulated acoustic emissions (CAEs) related to the total number of tracheids in Norway spruce (*Picea abies*) standard sections (13.3 mm longitudinal, 0.9 mm radial and 200 μm tangential) of different ages. Open circles, juvenile samples; closed squares, samples from the base of the crown; closed circles samples taken at 1 m from the ground. nE3, $n \times 10^{-3}$. ***, significant at the 0.001 level.

Europe PMC Funders Author Manuscripts

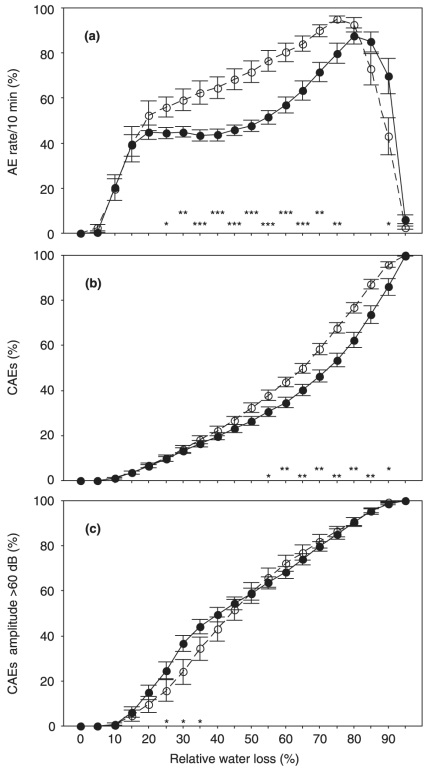

Fig. 3.

The rate of acoustic emissions per 10 minutes (AEs/10 min) related to maximum AEs/10 min (a), cumulated AEs related to the total number of AEs (b), and cumulated AEs with amplitudes > 60 dB related to the total number of AEs with these amplitudes (c) at 5% steps of relative water loss for juvenile (n = 12; open symbols, dashed lines) and mature Norway spruce (*Picea abies*) sapwood beams (n = 12; closed symbols, solid lines). Error bars represent 1 standard error. Differences between juvenile and mature samples are marked with * at the corresponding relative water loss if significant at the 0.05 level, with ** if significant at the 0.01 level, and with *** if significant at the 0.001 level.

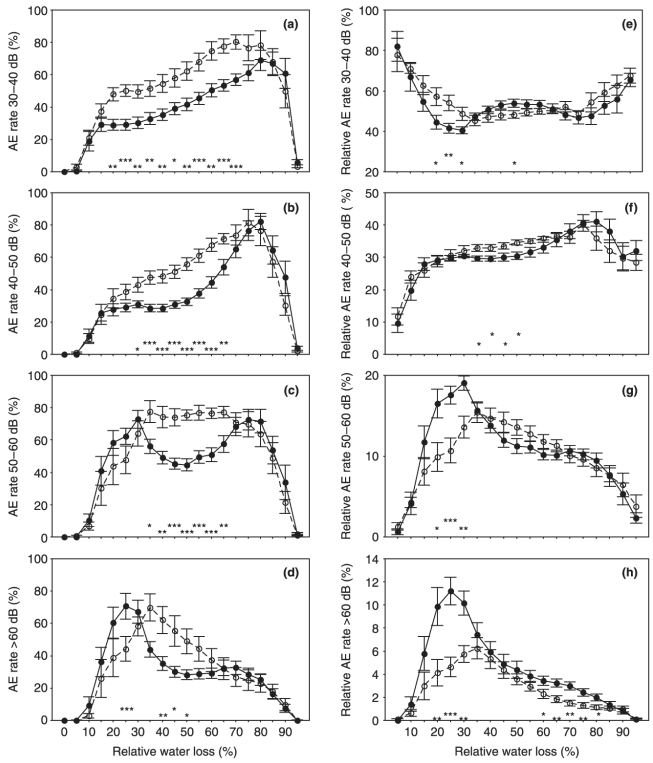

Fig. 4.

The acoustic emission rate per 10 minutes (AEs/10 min) related to maximum AEs/10 min (a–d) and the relative AE rate (AEs/10 min related to all AE signals detected at the same time interval) (e–g) clustered by the following peak amplitude (PA_{AE}) ranges: 30.5 dB ≤ PA_{AE} < 40 dB, 40 dB ≤ PA_{AE} < 50 dB, 50 dB ≤ PA_{AE} < 60 dB, and PA_{AE} ≥ 60 dB at 5% steps of relative water loss. Error bars represent 1 standard error. Significant differences between juvenile (open symbols, dashed lines; n = 12) and mature (closed symbols, solid lines; n = 12) Norway spruce (*Picea abies*) beams are marked with * at the corresponding relative water loss if significant at the 0.05 level, with ** if significant at the 0.01 level, and with *** if significant at the 0.001 level.

Europe PMC Funders Author Manuscripts

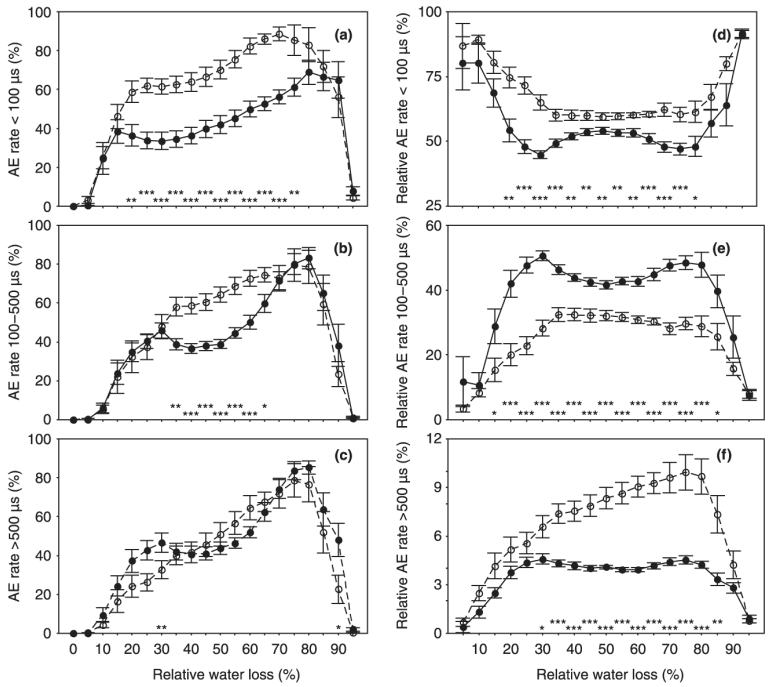

Fig. 5.

The acoustic emission rate per 10 minutes (AEs/10 min) related to maximum AEs/10 min (a–c) and the relative AE rate (AEs/10 min related to all AE signals detected at the same time interval) (d–f) clustered by the AE duration (D_{AE}) as follows: $D_{AE} < 100$ µs, 100 µs ≤ $D_{AE} < 500$ µs, and $D_{AE} \geq 500$ µs, at 5% steps of relative water loss. Error bars represent 1 standard error. Significant differences between juvenile (open symbols, dashed lines; $n = 12$) and mature (closed symbols, solid lines; $n = 12$) Norway spruce (*Picea abies*) beams are marked with * at the corresponding relative water loss if the difference is significant at the 0.05 level, with ** if it is significant at the 0.01 level, and with *** if it is significant at the 0.001 level.

Europe PMC Funders Author Manuscripts

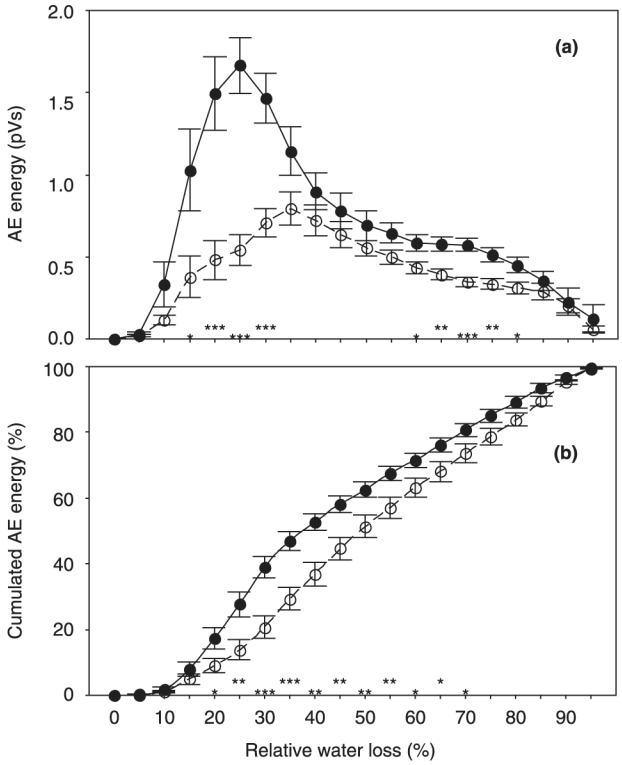

Fig. 6.

Mean relative acoustic emission (AE) energy per 10 min (pVs) (a) and relative cumulated AE energy (cumulated AE energy emitted until a defined RWL step related to the total AE energy) (b) at 5% relative water loss steps. Significant differences between juvenile (open symbols, dashed lines; $n = 12$) and mature (closed symbols, solid lines; $n = 12$) Norway spruce (*Picea abies*) beams are marked with * at the corresponding relative water loss if significant at the 0.05 level, with ** if significant at the 0.01 level, and with *** if significant at the 0.001 level. Error bars represent 1 standard error.

Europe PMC Funders Author Manuscripts

Table 1

Cumulated acoustic emissions (CAEs) clustered by waveform features, total acoustic emissions (AEs) and tracheid counts for Norway spruce (*Picea abies*) standard beams

	CAE 30.5–40 dB (%)	**CAE 40–50 dB (%)**	**CAE 50–60 dB (%)**	**CAE > 60 dB (%)**	**CAE < 100 µs (%)**	**CAE 100–500 µs (%)**	**CAE > 500 µs (%)**	**Total AEs (*n*)**	**Tracheids (*n* mm^{-2})**
Juvenile	52.16[a] (1.21)	34.73[a] (0.62)	10.55[a] (0.49)	2.55[a] (0.22)	63.43[a] (1.05)	28.29[a] (1.05)	8.20[a] (0.48)	1679512.0[a] (77032.9)	1393.1[a] (62.0)
Mature	51.70[a] (1.41)	34.52[a] (1.17)	10.22[a] (0.36)	3.55[b] (0.23)	54.84[b] (1.25)	41.33[b] (1.20)	3.83[b] (0.10)	567051.3[b] (18281.4)	795.5[b] (46.2)

CAEs clustered by four peak amplitude and three duration steps expressed as per cent of all acoustic signals, total numbers of acoustic emissions (total AEs) and the number of earlywood tracheids mm^{-2} transverse surface (‘Tracheids’) are given as mean and standard error (in parentheses). Significant differences at the 1% level (at least) between juvenile ($n = 12$) and mature ($n = 12$) trunkwood samples are indicated by different letters.